



# CHORUS

This is the accepted manuscript made available via CHORUS. The article has been published as:

## Ferromagnetic insulating state in tensile-strained LaCoO<sub>3</sub> thin films from LDA + U calculations

Han Hsu, Peter Blaha, and Renata M. Wentzcovitch

Phys. Rev. B **85**, 140404 — Published 11 April 2012

DOI: [10.1103/PhysRevB.85.140404](https://doi.org/10.1103/PhysRevB.85.140404)

# Ferromagnetic insulating state in tensile-strained LaCoO<sub>3</sub> thin films

Han Hsu,<sup>1</sup> Peter Blaha,<sup>2</sup> and Renata M. Wentzcovitch<sup>1</sup>

<sup>1</sup>*Department of Chemical Engineering and Materials Science,  
University of Minnesota, Minneapolis, Minnesota, USA*

<sup>2</sup>*Institute of Materials Chemistry, Vienna University of Technology,  
A-1060 Vienna, Getreidemarkt 9/165-TC, Austria*

(Dated: February 27, 2012)

With local density approximation + Hubbard  $U$  (LDA+ $U$ ) calculations, we show that the ferromagnetic (FM) insulating state observed in tensile-strained LaCoO<sub>3</sub> epitaxial thin films is most likely a mixture of low-spin (LS) and high-spin (HS) Co, namely, a HS/LS mixture state. Compared with other FM states, including the intermediate-spin (IS) state (*metallic* within LDA+ $U$ ), which consists of IS Co only, and the insulating IS/LS mixture state, the HS/LS state is the most favorable one. The FM order in HS/LS state is stabilized via the superexchange interactions between adjacent LS and HS Co. We also show that Co spin state can be identified by measuring the electric field gradient (EFG) at Co nucleus via nuclear magnetic resonance (NMR) spectroscopy.

PACS numbers: 75.50.Cc, 75.70.Ak, 76.60.Gv

Perovskite-structure oxides have been proven a fertile area in condensed matter physics. They exhibit amazing properties, including ferroelectricity, ferromagnetism, colossal magnetoresistance (CMR), and multiferroics (simultaneous ferroelectricity and ferromagnetism), as a consequence of their spin, lattice, charge, and orbital degree of freedom. Advances in thin-film growth techniques have even brought more promising potentials for their future application, as their properties can be engineered via epitaxial strains. A few examples include strontium titanate ( $\text{SrTiO}_3$ ), ferroelectric in tensile-strained thin film while paraelectric in bulk,<sup>1</sup> lanthanum titanate ( $\text{LaTiO}_3$ ), conducting in compressive-strained thin film while insulating in bulk,<sup>2</sup> and Europium titanate ( $\text{EuTiO}_3$ ), in which multiferroics induced by tensile strains has been observed.<sup>3</sup> As to lanthanum cobaltite ( $\text{LaCoO}_3$ ), a diamagnetic insulator in bulk at low temperatures ( $T < 35$  K), a ferromagnetic (FM) *insulating* state has been observed in tensile-strained thin films, e.g.  $\text{LaCoO}_3$  grown on  $\text{SrTiO}_3$  or  $(\text{LaAlO}_3)_{0.3}(\text{Sr}_2\text{AlTaO}_6)_{0.7}$ , at  $T < 85$  K,<sup>4-13</sup> while the ferromagnetism induced by compressive strains, e.g.  $\text{LaCoO}_3$  grown on  $\text{LaAlO}_3$ , is not conclusive.<sup>5-7,14</sup> Two questions arise immediately: (1) Given that there are six  $3d$  electrons in  $\text{Co}^{3+}$ , which can thus have a total electron spin  $S = 0, 1, \text{ or } 2$ , referred to as low-spin (LS), intermediate-spin (IS), and high-spin (HS) state, respectively, what is the spin state of Co in FM  $\text{LaCoO}_3$  thin films, in contrast to the LS Co in diamagnetic bulk? (2) What leads to the formation of FM order in  $\text{LaCoO}_3$  thin films? After all, FM *insulators* are rarely seen. So far, all first-principles calculations have only found FM *metallic*  $\text{LaCoO}_3$  thin films with all Co ions in IS state,<sup>11,15,16</sup> a prediction clearly inconsistent with transport measurements.<sup>6</sup>

While finite Co spin induced by tensile strains in  $\text{LaCoO}_3$  thin films has just started attracting attention, finite Co spin induced by thermal excitation in bulk  $\text{LaCoO}_3$  has been a highly controversial issue for decades.<sup>17,18</sup> With LS Co at  $T < 35$  K, bulk  $\text{LaCoO}_3$  becomes a paramagnetic insulator with finite Co spin at about 90 K. Such a spin-state crossover in the temperature range of 35–90 K was first suggested to be a LS-HS crossover<sup>19-21</sup> but was later suggested to be LS-IS based on a local density approximation + Hubbard  $U$  (LDA+ $U$ ) calculation.<sup>22</sup> Since then, both scenarios have received supports from various experimental and theoretical works, but a consensus is not yet achieved (see Ref. 23 for a brief review). A study regarding  $\text{LaCoO}_3$  thin films may also help understanding  $\text{LaCoO}_3$  bulk from a different perspective. In this paper, we investigate the Co spin state in tensile-strained thin films and the formation of FM order via a series of LDA+ $U$  calculations. While LDA+ $U$  has been frequently used to study cobaltites and Co spin state, the choice of Hubbard  $U$  can be an issue. It has been shown that under the same lattice parameter, the Hubbard  $U$  affects the total energy and the determination of ground state.<sup>16</sup> A well justified Hubbard  $U$  determined by first principles would thus be necessary for finding out the the actual ground state. In this paper, we compute the Hubbard  $U$  parameters of Co in all spin states self-consistently with a linear response approach.<sup>24-26</sup> This method has successfully found the ground state of iron-bearing magnesium silicate ( $\text{MgSiO}_3$ ) perovskite at a wide range of pressure.<sup>26</sup> Both the plane-wave pseudopotential (PWPP) method<sup>27</sup> implemented in QUANTUM ESPRESSO codes<sup>28</sup> and the augmented plane wave + local orbitals (APW+lo) method<sup>29</sup> implemented in WIEN2k codes<sup>30</sup> are used. As shall be pointed out later, the orbital occupancies of Co in thin films are different from those in bulk, due to their different symmetries. We therefore compute the electric field gradient (EFG) tensor at Co nucleus,  $V_{zz}$ , with WIEN2k, to see whether the Co spin state in thin films can be identified via EFG, as demonstrated in bulk.<sup>23</sup>

The pseudocubic lattice parameter of bulk  $\text{LaCoO}_3$  ( $R\bar{3}c$  symmetry) is about 3.81 Å at  $T \sim 5$  K.<sup>31,32</sup> To model tensile-strained  $\text{LaCoO}_3$  thin films via bulk calculations, we constrain the in-plane pseudocubic lattice parameters  $a_{\text{pc}}$  and  $b_{\text{pc}}$  of the hypothetical bulk to 3.899 Å (the lattice constant of cubic  $\text{SrTiO}_3$  at low temperatures),<sup>33</sup> set  $\alpha = \beta = \gamma = 90^\circ$ , and optimize the out-of-plane pseudocubic lattice parameter ( $c_{\text{pc}}$ ). Due to the lack of accurate information regarding  $\text{CoO}_6$  octahedral rotation in thin-film  $\text{LaCoO}_3$  in the low-temperature FM phase, we consider two extreme cases shown in Fig. 1: (a) cube-on-cube, namely, no  $\text{CoO}_6$  octahedral rotation degree of freedom, and (b) full  $\text{CoO}_6$  rotation degree of freedom subject to the above-mentioned constraints. We also consider several magnetic configurations shown in Fig. 2: (a) all Co ions in LS state, (b) all Co ions have the same magnetic moment aligned in FM order, and (c) a mixture state with LS Co surrounded by magnetic Co (and vice versa) aligned in FM order. The configuration shown in Fig. 2(c) is a legitimate postulate, as the observed magnetization in  $\text{LaCoO}_3$  thin films rarely exceeds  $0.85 \mu_B/\text{Co}$ .<sup>4-11</sup> For the configuration in Fig. 2(b), a convergent wave function for HS state cannot be obtained; only IS state can be found. For the configuration in Fig. 2(c), both HS/LS and IS/LS mixture state can be obtained. The self-consistent Hubbard  $U$  parameter ( $U_{\text{sc}}$ ) of LS and IS Co are 7.0 eV, while the HS/LS state has  $U_{\text{sc}}^{(\text{HS})} = 5.4$  and  $U_{\text{sc}}^{(\text{LS})} = 7.2$  eV.<sup>34</sup> The dependence of  $U_{\text{sc}}$  on  $c_{\text{pc}}$  is negligible. To demonstrate how the choice of Hubbard  $U$  can affect the determination of ground state, we also present the result obtained using a constant  $U = 7$  eV for all Co in our PWPP calculations. In tensile-strained  $\text{LaCoO}_3$  thin films,  $\text{CoO}_6$  octahedra possess tetragonal symmetry, namely, longer Co–O distance on the  $xy$  plane, regardless of  $\text{CoO}_6$  rotation, as will be discussed in the next paragraph. In tetragonal symmetry ( $D_{4h}$ ), the spin-down electron of HS Co occupies  $d_{xy}$  orbital, and the spin-down electrons of IS Co occupy  $d_{xz}$  and  $d_{yz}$  orbitals, as shown in Fig. 2(d). Such orbital occupancies are very different from those in bulk  $\text{LaCoO}_3$ , in which  $\text{CoO}_6$  octahedra have trigonal symmetry ( $D_{3d}$ ), with the [111] direction being the

high-symmetry axis. In bulk LaCoO<sub>3</sub>, the spin-down electron of HS Co occupies the  $d_{z^2}$ -like orbital oriented along the [111] direction, and the IS Co spin-down electrons occupy the doublet with 3-fold rotation symmetry about the [111] direction.<sup>23</sup>

The optimized out-of-plane pseudocubic lattice parameter ( $c_{pc}$ ) of each FM state and associated relative energy ( $\Delta E$ ) and band gap ( $E_{gap}$ ) are listed in Tables I-II. Regardless of CoO<sub>6</sub> rotation, the HS/LS mixture state (with  $U_{sc}$ ) is the most stable FM state given by the PWPP method (Table I).<sup>35</sup> While the choice of  $U = 7.0$  eV makes HS/LS state less favorable in PWPP calculations, APW+lo calculations still find HS/LS the most stable FM state (Table II). Both PWPP and APW+lo methods open an energy gap for HS/LS state, consistent with transport measurements.<sup>6</sup> Also, the presence of HS Co is consistent with recent x-ray magnetic circular dichroism (XMCD) and x-ray absorption spectroscopy (XAS) spectra.<sup>9,10</sup> In contrast, the IS state is never the most favorable FM state, regardless of the computation method and CoO<sub>6</sub> rotation. Its partially filled bands formed by partially occupied  $d_{z^2}$  and  $d_{x^2-y^2}$  orbitals in IS Co lead to a nonzero density of state at the Fermi level. When the IS Co concentration is reduced to 50%, an energy gap is opened in APW+lo calculations (Table II), while PWPP calculations still give a conducting IS/LS state (Table I). Such a difference is likely to result from the way that the Hubbard  $U$  is applied. In PWPP, the Hubbard  $U$  is applied to the projection of the total wave function onto Co 3d orbitals;<sup>24</sup> in APW+lo, the Hubbard  $U$  is directly applied to the 3d orbitals within the muffin-tin radius of Co (1.9 bohr). Insulating or not, the IS/LS state is highly unlikely; its energy is even higher than that of IS state. One more thing worthy of mention is that the Co–O distance ( $d_{Co-O}$ ) and Co–O–Co angle obtained in our calculation are different from those estimated in Ref. 5, where a constant  $d_{Co-O} = 1.93$  Å is assumed (regardless of compressive or tensile strains), and an Co–O–Co angle of 176° is estimated for LaCoO<sub>3</sub> grown on SrTiO<sub>3</sub>. In our PWPP calculation with  $U_{sc}$  and CoO<sub>6</sub> rotation, the HS/LS state has  $d_{Co(HS)-O} = 2.015$  and 1.872 Å,  $d_{Co(LS)-O} = 1.922$  and 1.886 Å, and Co–O–Co angles of 163.8° and 156.6°, on the  $xy$  plane and along the  $z$  axis, respectively. Even for the IS state suggested by Ref. 5, we have  $d_{Co(IS)-O} = 1.973$  and 1.939 Å, and Co–O–Co angles of 162.3° and 154.9°, on the  $xy$  plane and along the  $z$  axis, respectively.

Other than the total energy, structural properties can be a useful criterion to determine which FM state favors tensile strains ( $c_{pc}/a_{pc} < 1$ ). Starting with the structures listed in Table I with CoO<sub>6</sub> rotation, we perform full structural optimization (at constrained volume) via variable cell-shape damped molecular dynamics.<sup>36</sup> All lattice parameters, including  $\alpha$ ,  $\beta$ , and  $\gamma$ , are optimized, so the final structures only experience hydrostatic pressures. With  $\alpha$ ,  $\beta$ , and  $\gamma$  slightly deviated from 90°, the IS state has  $c_{pc}/a_{pc} > 1$ , while all other states remain  $c_{pc}/a_{pc} < 1$  (but IS/LS state still has a  $c_{pc}/a_{pc}$  larger than that of HS/LS state), as shown in Table III. The larger  $c_{pc}/a_{pc}$  ratio associated with IS Co is a direct consequence of its occupied  $d_{xz}$  and  $d_{yz}$  orbitals (by spin-down electrons), which elongate the Co–O distance along the  $z$ -direction. In contrast, the fully optimized HS/LS state has  $c_{pc}/a_{pc} = 0.969$ , in great agreement with  $c_{pc}/a_{pc} = 0.967$  observed in experiments.<sup>6</sup>

A significant part of cobalt-spin controversy arises from the difficulty in directly measuring the total electron spin of Co. Such difficulty, also appearing in other spin systems, can be resolved by comparing the calculated and measured EFGs.<sup>23,26,37</sup> So far, insulating FM state has been observed in LaCoO<sub>3</sub> thin films with  $a_{pc}$  ranging from 3.84 to 3.90 Å.<sup>5,8</sup> In these thin films, the magnetic Co concentration and Co–O distance may be different, which can lead to slightly different EFG for Co in the same spin state. To find out possible upper and lower limits of HS and IS Co EFG, we compute them in two extreme cases: (1) thin films with  $a_{pc} = 3.899$  Å and 50% of magnetic Co, namely, the HS/LS and IS/LS states listed in Tables I and II, and (2) single isolated HS or IS Co in an array of LS Co in a fully relaxed structure with  $a_{pc} \sim 3.81$  Å, where the orbital occupancies of isolated HS and IS Co are maintained in tetragonal symmetry [Fig. 2(d)]. In these APW+lo calculations, IS Co does not lead to a metallic state, in contrast to bulk LaCoO<sub>3</sub> ( $D_{3d}$  symmetry).<sup>23</sup> Different choices of Hubbard  $U$  have been adopted as well (5 eV, 7 eV, and  $U_{sc}$ ). The results of all these calculations show that the EFG mainly depends on the spin state:  $14.7 < V_{zz}^{(HS)}/(10^{21} \text{ V/m}^2) < 19.9$  and  $-14.6 < V_{zz}^{(IS)}/(10^{21} \text{ V/m}^2) < -8.0$ . The quadrupole frequency,  $\nu_Q \equiv 3eQ|V_{zz}|/2I(2I-1)h$ , can thus be easily predicted, with  $Q = 0.42 \times 10^{-28} \text{ m}^2$  and  $I = 7/2$  for <sup>59</sup>Co nucleus. Based on the range of  $V_{zz}^{(HS)}$  and  $V_{zz}^{(IS)}$ , we conclude that in insulating LaCoO<sub>3</sub> thin films, a measured  $\nu_Q$  via nuclear magnetic resonance (NMR) spectroscopy within  $\sim 8.2 \pm 2.4$  MHz can be a strong evidence for IS Co, and a measured  $\nu_Q$  within  $\sim 12.6 \pm 1.9$  MHz should indicate HS Co.

Analysis of electronic structures can help developing a physical understanding for the FM order in HS/LS state, whose projected density of states (PDOS) are shown in Fig. 3. The case with  $U = 7$  eV and no CoO<sub>6</sub> rotation is presented, as the main features in PDOS are not sensitive to the choice of  $U$  and CoO<sub>6</sub> rotation. Extracted from Fig. 3(a), both HS and LS Co have nonzero magnetic moment: 2.97 and 0.56  $\mu_B$ , respectively. The FM order is established via the superexchange interaction between HS and LS Co, as described by the Goodenough-Kanamori

126 rule,<sup>17,38–40</sup> which states that the superexchange interaction between two cations (with or without a shared anion) is  
 127 ferromagnetic if the electron transfer is from a filled to a half-filled orbital or from a half-filled to an empty orbital.  
 128 Indeed, for the HS/LS state, electrons transfer from the filled  $d_{xz}$  and  $d_{yz}$  orbitals of LS Co to the half-filled  $d_{xz}$  and  
 129  $d_{yz}$  orbitals of HS Co via the oxygen in between, and also from the half-filled  $e_g$  ( $d_{z^2}$  and  $d_{x^2-y^2}$ ) orbitals of HS Co  
 130 to the empty  $e_g$  orbitals of LS Co, as depicted in the inset of Fig. 3(b). The PDOS shown in Fig. 3(b) confirms this  
 131 model: the finite spin-up  $e_g$  electrons localized at the LS Co site (transferred from the HS Co site) and the finite  
 132 spin-down  $d_{xz}$  and  $d_{yz}$  electrons localized at the HS Co site (transferred from the LS Co site). Such electron transfers  
 133 have been also described via a *configuration fluctuation* model,<sup>20,21</sup> which further suggests that the interchange of  
 134 spin states (without net transfer of charge) led by electron transfers stabilizes the FM order in this HS/LS states.

135 The above-mentioned superexchange interaction can be visualized via electron spin density  $s(\mathbf{r}) \equiv \rho_{\uparrow}(\mathbf{r}) - \rho_{\downarrow}(\mathbf{r})$ ,  
 136 where  $\rho_{\uparrow}(\mathbf{r})$  and  $\rho_{\downarrow}(\mathbf{r})$  are spin-up and spin-down electron density, respectively. Figure 4(a) shows  $s(\mathbf{r})$  corresponding  
 137 to the configuration with all HS Co magnetic moments aligned (same as the configuration in Fig. 3). The nonzero  
 138 magnetic moments localized at LS Co sites (with  $e_g$  character), aligned with the HS Co magnetic moments, are  
 139 consistent with the PDOS shown in Fig. 3. When the magnetic moment of one HS Co in a 40-atom supercell is  
 140 flipped [Fig. 4(b)], the alignment of magnetic moments is altered, and so is the condition that allows configuration  
 141 fluctuation [inset of Fig. 3(b)]. The spin density at surrounding LS Co sites is thus significantly affected. One flipped  
 142 HS Co spin (in a 40-atom cell) increases the total energy by 195 meV/supercell. Flipping one more HS Co spin, so  
 143 the total magnetization per supercell becomes zero, further increases the total energy by 78 meV/supercell. With  
 144  $\text{CoO}_6$  rotation, the energy increases associated with one and two flipped HS Co spins are 96 and 34 meV/supercell,  
 145 respectively. These results indicates that the magnetic moment of HS Co in the HS/LS state should align at low  
 146 temperatures.

147 While our calculations have shown that HS/LS state is the most favorable state among the ferromagnetic states  
 148 being considered, magnetic state in actual  $\text{LaCoO}_3$  thin films can be more complicated. The magnetization observed in  
 149 experiments rarely exceeds  $0.85 \mu_B/\text{Co}$ ,<sup>4–11</sup> smaller than that of the HS/LS mixture ( $2 \mu_B/\text{Co}$ ). Such a magnetization  
 150 suggests that the HS Co population should be smaller than 50%. In fact, XAS spectra combined with atomic multiplet  
 151 calculations have suggested that  $\text{LaCoO}_3$  thin film on  $\text{SrTiO}_3$  consists of about 64% of LS Co and 36% of HS Co.<sup>10</sup>  
 152 Given that the FM order is achieved via the superexchange interaction within the HS-LS-HS Co configuration shown  
 153 in Fig. 2(c), one can thus expect ferromagnetic HS/LS domain and nonmagnetic LS domain coexist in tensile strained  
 154 thin films, as observed using magnetic force microscopy (MFM).<sup>7</sup> Also, since HS/LS state favors larger in-plane lattice  
 155 parameter, thin films with larger in-plane lattice parameters can be expected to have larger HS/LS domain, and thus  
 156 larger magnetization, consistent with the increase of magnetization with lattice parameter observed in experiment.<sup>5</sup>

157 In summary, we use LDA+ $U$  calculations to show that the ferromagnetic insulating state in tensile-strained  $\text{LaCoO}_3$   
 158 thin films is most likely a mixture of HS and LS Co. Among all the ferromagnetic states studied in this paper (HS/LS,  
 159 IS/LS, and IS), the insulating HS/LS mixture state is the most favorable one, energetically and structurally. Its FM  
 160 order is established via the superexchange interaction between LS and HS Co. We also show that cobalt spin states  
 161 in  $\text{LaCoO}_3$  thin films could be identified via NMR spectroscopy.

162 This work was primarily supported by the MRSEC Program of NSF grants DMR-0212302 and DMR-0819885, and  
 163 partially supported by EAR-081272 and EAR-1047629. P.B. was supported by the Austrian Science Fund (SFB F41,  
 164 "ViCoM"). Calculations were performed at the Minnesota Supercomputing Institute (MSI). We thank C. Leighton  
 165 for valuable discussions.

- 
- 166 <sup>1</sup> J. H. Haeni *et al.*, Nature **430**, 758 (2004).  
167 <sup>2</sup> F. J. Wong *et al.*, Phys. Rev. B **81**, 161101(R) (2010).  
168 <sup>3</sup> J. H. Lee *et al.*, Nature **466**, 954 (2010).  
169 <sup>4</sup> D. Fuchs *et al.*, Phys. Rev. B **75**, 144402 (2007).  
170 <sup>5</sup> D. Fuchs *et al.*, Phys. Rev. B **77**, 014434 (2008).  
171 <sup>6</sup> J. W. Freeland *et al.*, Appl. Phys. Lett. **93**, 212501 (2008).  
172 <sup>7</sup> S. Park *et al.*, Appl. Phys. Lett. **95**, 072508 (2009).  
173 <sup>8</sup> A. Herklotz *et al.*, Phys. Rev. B **79**, 092409 (2009).  
174 <sup>9</sup> V. V. Mehta *et al.*, J. Appl. Phys. **105**, 07E503 (2009).  
175 <sup>10</sup> M. Merz *et al.*, Phys. Rev. B **82**, 174416 (2010).  
176 <sup>11</sup> A. Posadas *et al.*, Appl. Phys. Lett. **98**, 053104 (2011).  
177 <sup>12</sup> C. Pinta *et al.*, Phys. Rev. B **78**, 174402 (2008).  
178 <sup>13</sup> D. Fuchs *et al.*, Phys. Rev. B **79**, 024424 (2009).  
179 <sup>14</sup> V. Mehta and Y. Suzuki, J. Appl. Phys. **109**, 07D717 (2011).  
180 <sup>15</sup> K. Gupta and P. Mahadevan, Phys. Rev. B **79**, 020406(R) (2009).  
181 <sup>16</sup> J. M. Rondinelli and N. A. Spaldin, Phys. Rev. B **79**, 054409 (2009).  
182 <sup>17</sup> J. B. Goodenough, *Localized to Itinerant Electronic Transition in Perovskite Oxides* (Springer, 2001).  
183 <sup>18</sup> C. N. R. Rao *et al.*, Top. Curr. Chem. **234**, 1 (2004).  
184 <sup>19</sup> P. M. Raccach and J. B. Goodenough, Phys. Rev. **155**, 932 (1967).  
185 <sup>20</sup> M. A. Se nar s-Rodr guez and J. B. Goodenough, J. Solid State Chem. **116**, 224 (1995).  
186 <sup>21</sup> M. A. Se nar s-Rodr guez and J. B. Goodenough, J. Solid State Chem. **118**, 323 (1995).  
187 <sup>22</sup> M. A. Korotin *et al.*, Phys. Rev. B **54**, 5309 (1996).  
188 <sup>23</sup> Han Hsu *et al.*, Phys. Rev. B **82**, 100406(R) (2010).  
189 <sup>24</sup> M. Cococcioni and S. de Gironcoli, Phys. Rev. B **71**, 035105 (2005).  
190 <sup>25</sup> V. L. Campo Jr and M. Cococcioni, J. Phys.: Condens. Matter **22**, 055602 (2010).  
191 <sup>26</sup> Han Hsu *et al.*, Phys. Rev. Lett. **106**, 118501 (2011).  
192 <sup>27</sup> Pseudopotentials used in this paper have been reported in H. Hsu *et al.*, Phys. Rev. B **79**, 125124 (2009).  
193 <sup>28</sup> P. Giannozzi *et al.*, J. Phys.: Condens. Matter **21**, 395502 (2009).  
194 <sup>29</sup> G. Madsen *et al.*, Phys. Rev. B **64**, 195134 (2001).  
195 <sup>30</sup> P. Blaha *et al.*, *WIEN2k, An Augmented Plane Wave Plus Local Orbitals Program for Calculating Crystal Properties*, edited  
196 by K. Schwarz, Techn. Universit t Wien, Vienna (2001).  
197 <sup>31</sup> P. G. Radaelli and S.-W. Cheong, Phys. Rev. B **66**, 094408 (2002).  
198 <sup>32</sup> While LDA+ $U$  gives a pseudocubic lattice parameter of about 3.78   for bulk LaCoO<sub>3</sub> (see Ref. 27), inclusion of zero point  
199 motion energy can improve this 1% underestimate, and better agreement with experiments can be achieved, as reviewed by  
200 R. M. Wentzcovitch *et al.*, Rev. Min. Geochem. **71**, 59 (2010).  
201 <sup>33</sup> F. W. Lytle, J. Appl. Phys. **35**, 2212 (1964).  
202 <sup>34</sup> In this paper,  $U_{sc}$  is extracted from a series of LDA+ $U$  ground states associated with different trial  $U$ , as detailed in the  
203 supplemental material of Ref. 26 (<http://link.aps.org/supplemental/10.1103/PhysRevLett.106.118501>). In our earlier work  
204 on LS LaCoO<sub>3</sub> (Ref. 27), the Hubbard  $U$  for LS Co ( $\sim 8.3$  eV) was extracted from the LDA ground state, as detailed in  
205 Ref. 24.  
206 <sup>35</sup> In our calculations with constrained in-plane lattice parameters ( $a_{pc} = b_{pc} = 3.899$   ), a HS state with G-type antiferro-  
207 magnetic (AFM) order can be obtained, and its energy is lower than that of the HS/LS state. Given the neglect of finite  
208 thickness, the possible uncertainty of energy given by LDA+ $U$  method, and the fact that AFM thin film is not observed in  
209 experiments, we limit our discussions on the available FM states (IS, IS/LS, and HS/LS).  
210 <sup>36</sup> R. M. Wentzcovitch *et al.*, Phys. Rev. Lett. **70**, 3947 (1993).  
211 <sup>37</sup> Han Hsu *et al.*, Earth Planet. Sci. Lett. **294**, 19 (2010).  
212 <sup>38</sup> J. B. Goodenough, Phys. Rev. **100**, 564 (1955).  
213 <sup>39</sup> J. B. Goodenough, J. Phys. Chem. Solids **6**, 287 (1958).  
214 <sup>40</sup> J. Kanamori, J. Phys. Chem. Solids **10**, 87 (1959).

TABLE I. Optimized out-of-plane pseudocubic lattice parameter ( $c_{pc}$ ) and associated relative energy ( $\Delta E$ ) and energy gap ( $E_{gap}$ ) of each FM state in tensile-strained  $\text{LaCoO}_3$  thin film (PWPP method).

	No $\text{CoO}_6$ rotation			Full $\text{CoO}_6$ rotation		
	$c_{pc}$ ( $\text{\AA}$ )	$\Delta E$ (eV/f.u.)	$E_{gap}$ (eV)	$c_{pc}$ ( $\text{\AA}$ )	$\Delta E$ (eV/f.u.)	$E_{gap}$ (eV)
LS	3.865	0.35	0.54	3.660	0.32	1.24
IS	3.785	0.20	metal	3.785	0.19	metal
IS/LS	3.720	0.35	metal	3.680	0.29	metal
HS/LS ( $U_{sc}$ )	3.685	0.00	0.92	3.680	0.00	0.90
HS/LS ( $U = 7$ eV)	3.700	0.29	1.12	3.695	0.29	0.90

TABLE II. Optimized  $c_{pc}$  and associated  $\Delta E$  and  $E_{gap}$  of each FM state (APW+lo method, with  $\text{CoO}_6$  rotation).

	$c_{pc}$ ( $\text{\AA}$ )	$\Delta E$ (eV/f.u.)	$E_{gap}$ (eV)
LS	3.660	0.37	1.72
IS	3.741	0.18	metal
IS/LS	3.672	0.29	0.59
HS/LS ( $U = 7$ eV)	3.686	0	1.52

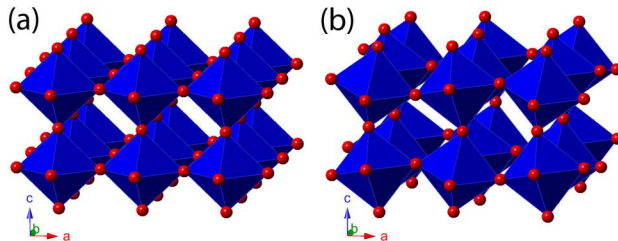


FIG. 1. (color online). Possible atomic structures of  $\text{LaCoO}_3$  thin film (La is not shown) subject to constrained in-plane lattice parameters. (a) Cube on cube, no  $\text{CoO}_6$  octahedral rotation; (b) full octahedral rotation degree of freedom.

TABLE III. Fully optimized pseudocubic lattice parameters of each FM state at the volume as in Table I (with  $\text{CoO}_6$  rotation).

	$a_{pc}, b_{pc}$ ( $\text{\AA}$ )	$c_{pc}$ ( $\text{\AA}$ )	$c_{pc}/a_{pc}$
IS	3.848	3.893	1.012
IS/LS	3.847	3.778	0.982
HS/LS ( $U_{sc}$ )	3.863	3.745	0.969
HS/LS ( $U = 7$ eV)	3.865	3.757	0.972

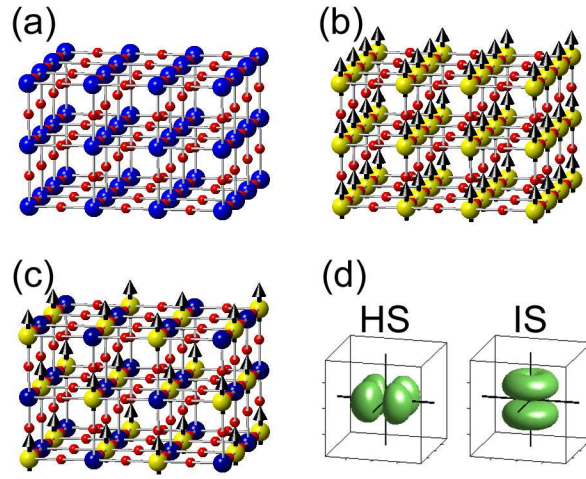


FIG. 2. (color online). (a)-(c) Possible magnetic configurations in LaCoO<sub>3</sub> epitaxial thin film (La is not shown). The arrows denote for nonzero magnetic moments, either IS or HS. (a) LS state; (b) HS or IS state in FM order; (c) HS/LS or IS/LS mixture state in FM order. (d) The 3d orbitals occupied by the spin-down electrons of HS and IS Co.

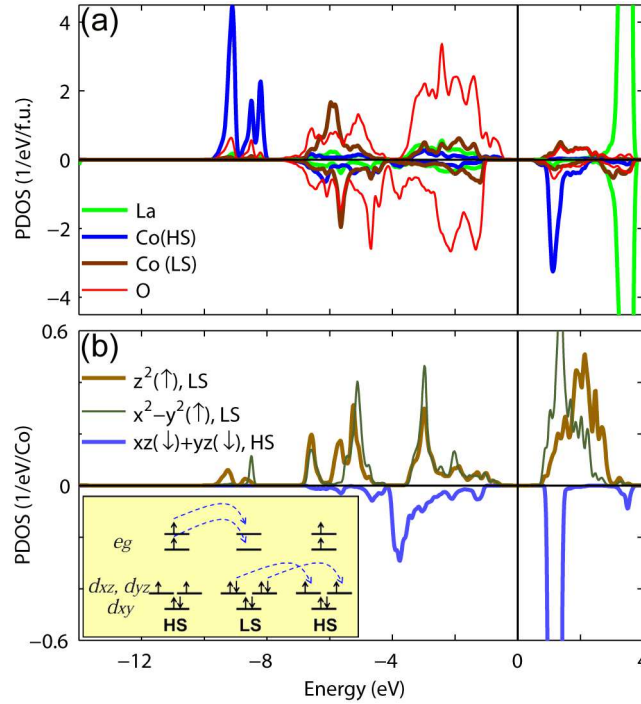


FIG. 3. (color online). Projected density of states of ferromagnetic HS/LS state (no CoO<sub>6</sub> rotation,  $U = 7$  eV) onto (a) each atomic site, and (b) some of the Co 3d orbitals. The inset in (b) shows the electron transfer between HS and LS Co.



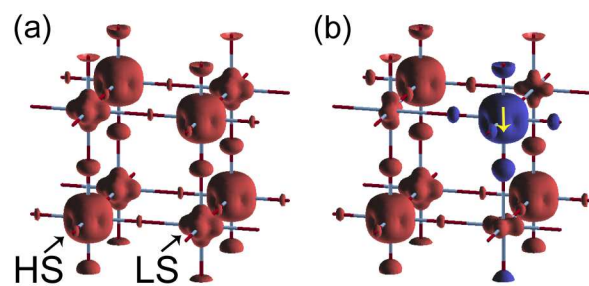


FIG. 4. (color online). Spin density,  $s(\mathbf{r})$ , of HS/LS state (no  $\text{CoO}_6$  rotation,  $U = 7$  eV) with (a) all HS Co magnetic moments aligned, and (b) one HS Co magnetic moment flipped downward (indicated by arrow). The isosurface values are 0.02 (red) and  $-0.02$  (blue).